
# NAVAL POSTGRADUATE SCHOOL

**MONTEREY, CALIFORNIA**

# THESIS

**DEVELOPMENT AND ANALYSIS OF A BI-DIRECTIONAL TIDAL TURBINE**

by

Jason K. Ponder

March 2012

| | |
|---|---|
| Thesis Advisor: | Garth Hobson |
| Second Reader: | Anthony Gannon |

THIS PAGE INTENTIONALLY LEFT BLANK

| REPORT DOCUMENTATION PAGE | | | Form Approved OMB No. 0704-0188 |
|---|---|---|---|
| Public reporting burden for this collection of information is estimated to average 1 hour per response, including the time for reviewing instruction, searching existing data sources, gathering and maintaining the data needed, and completing and reviewing the collection of information. Send comments regarding this burden estimate or any other aspect of this collection of information, including suggestions for reducing this burden, to Washington headquarters Services, Directorate for Information Operations and Reports, 1215 Jefferson Davis Highway, Suite 1204, Arlington, VA 22202-4302, and to the Office of Management and Budget, Paperwork Reduction Project (0704-0188) Washington DC 20503. | | | |
| **1. AGENCY USE ONLY** ***(Leave blank)*** | **2. REPORT DATE** March 2012 | **3. REPORT TYPE AND DATES COVERED** Master's Thesis | |
| **4. TITLE AND SUBTITLE** Development and Analysis of a Bi-Directional Tidal Turbine | | **5. FUNDING NUMBERS** | |
| **6. AUTHOR(S)** Jason K. Ponder | | | |
| **7. PERFORMING ORGANIZATION NAME(S) AND ADDRESS(ES)** Naval Postgraduate School Monterey, CA 93943-5000 | | **8. PERFORMING ORGANIZATION REPORT NUMBER** | |
| **9. SPONSORING /MONITORING AGENCY NAME(S) AND ADDRESS(ES)** N/A | | **10. SPONSORING/MONITORING AGENCY REPORT NUMBER** | |
| **11. SUPPLEMENTARY NOTES** The views expressed in this thesis are those of the author and do not reflect the official policy or position of the Department of Defense or the U.S. Government. IRB Protocol number _____N/A_____. | | | |
| **12a. DISTRIBUTION / AVAILABILITY STATEMENT** Approved for public release; distribution is unlimited | | **12b. DISTRIBUTION CODE** A | |

**13. ABSTRACT (maximum 200 words)**

The concept of using renewable energy for power generation has experienced much attention with increasing costs of non-renewable sources. The largest untapped renewable energy resource is in the form of the oceans and currents created by them. It has been proven that many different concepts and designs are possible for this use and this study will focus on a bi-directional turbine created for this purpose.

In the present study, the commercial CFD software ANSYS CFX was utilized to build a turbine map. The basic turbine map was developed for a 25 blade bi-axial turbine under various flow conditions and the optimal efficiency for each flow condition was determined and a further analysis of the number of blades in the rotor was completed. The flow diagrams produced by the CFD analysis show that many improvements can still be made to the design in future iterations.

| **14. SUBJECT TERMS** Cross-Flow, Tidal Turbine, Renewable Energy, Green Energy | | | **15. NUMBER OF PAGES** 69 |
|---|---|---|---|
| | | | **16. PRICE CODE** |
| **17. SECURITY CLASSIFICATION OF REPORT** Unclassified | **18. SECURITY CLASSIFICATION OF THIS PAGE** Unclassified | **19. SECURITY CLASSIFICATION OF ABSTRACT** Unclassified | **20. LIMITATION OF ABSTRACT** UU |

NSN 7540-01-280-5500

Standard Form 298 (Rev. 2-89)
Prescribed by ANSI Std. 239-18

THIS PAGE INTENTIONALLY LEFT BLANK

**Approved for public release; distribution is unlimited**

**DEVELOPMENT AND ANALYSIS OF A BI-DIRECTIONAL TIDAL TURBINE**

Jason K. Ponder
Lieutenant, United States Navy
B.S. Mechanical Engineering, United States Naval Academy, 2007

Submitted in partial fulfillment of the
requirements for the degree of

**MASTER OF SCIENCE IN MECHANICAL ENGINEERING**

from the

**NAVAL POSTGRADUATE SCHOOL**
**MARCH 2012**

Author: Jason K. Ponder

Approved by: Garth V. Hobson
Thesis Advisor

Anthony J. Gannon
Second Reader

Knox T. Millsaps
Chair, Department of Mechanical and Aerospace Engineering

THIS PAGE INTENTIONALLY LEFT BLANK

# ABSTRACT

The concept of using renewable energy for power generation has experienced much attention with increasing costs of non-renewable sources. The largest untapped renewable energy resource was in the form of the oceans and currents created by them. It has been proven that many different concepts and designs are possible for this use and this study will focus on a bi-directional turbine created for this purpose.

In the present study, the commercial CFD software ANSYS CFX was utilized to build a turbine map. The basic turbine map was developed for a 25 blade bi-axial turbine under various flow conditions and the optimal efficiency for each flow condition was determined and a further analysis of the number of blades in the rotor was completed. The flow diagrams produced by the CFD analysis show that many improvements can still be made to the design in future iterations.

THIS PAGE INTENTIONALLY LEFT BLANK

# TABLE OF CONTENTS

THIS PAGE INTENTIONALLY LEFT BLANK

# LIST OF FIGURES

THIS PAGE INTENTIONALLY LEFT BLANK

# LIST OF TABLES

THIS PAGE INTENTIONALLY LEFT BLANK

# ACKNOWLEDGMENTS

I would like to express my appreciation to the following people whose valuable contribution aided to the completion of this thesis.

Professor Garth Hobson, his patient support and professional instruction throughout the entire process made my study possible.

Dr. Anthony Gannon's analytical abilities aided in the creation of the CFD analysis and troubleshoot the problems that arose.

My girlfriend, Cecelia Arkenbout, who was infinitely patient and supportive throughout the many late nights of studies.

Finally, I would like to thank my family. My mother, Frances, who pushed to keep me focused. My father, Keith, who kept things in perspective. My brother, Aaron, who made sure I had fun while I enjoyed my time in Monterey.

THIS PAGE INTENTIONALLY LEFT BLANK

# I. INTRODUCTION

As renewable energy markets continue to grow some resources have been reconsidered as a viable source for electrical power generation. Society has used the power found within moving water longer than it has been used any other power source. Wind, coal, and oil were used for their energy capabilities long after the first water powered turbines dating back to the 1st century BC in the Roman Empire [1]. Since that time, society's needs for convenient energy and power has shifted to new technologies such as coal, oil, natural gas, and most recently nuclear power. However, the ability of technology to keep up with the needs of society without putting unreasonable stress on the environment is not yet possible. Innovative methods for power production must be exploited. There are many possibilities in reverting to the origins of power production and focusing on the most powerful force on the planet, the oceans.

Hydropower has always been a key resource throughout civilization. Most towns and cities are built around waterways that were utilized for grain production and, as turbine technology developed, electric lighting. Cross-flow turbines have been used for hydropower as an effective way of creating power from the water flow. Many cascade design configurations have been tested [2], but a bi-directional cross-flow design has not been researched. A cascade mono-directional cross-flow design developed by the University of Clemson [3] provided the basis of design to create a bi-directional turbine. By creating the bi-directional turbine, the system could be used in power dense oceans and tidal streams.

Tidal flow has always been viewed as a great source for power generation. The problem has always been efficiently harnessing that power and getting it from source to consumer. Over the last fifty years, several tidal turbine designs have been created by a variety of companies from around the world. Many of these designs are either installed, or in the process of being installed. The designs range from a tidal barrage, twin propellers, three-bladed propellers similar to wind turbines, ducted propellers, a vertical axis turbine, and many other variations of these designs.

A tidal barrage [4] is currently the most common form of tidal power augmentation and relies on a large dam that funnels the water into the generation plant and through a large turbine as the tide flows in and out.

Figure 1 Annapolis Tidal Power Plant in Nova Scotia, Canada (From [4])

A second design is a twin bladed propeller [5] that will be the world's largest tidal device created by Marine Current Turbines. It will turn at a rate of ten to twenty revolutions per minute and produce over 1.2 Megawatts of electricity.

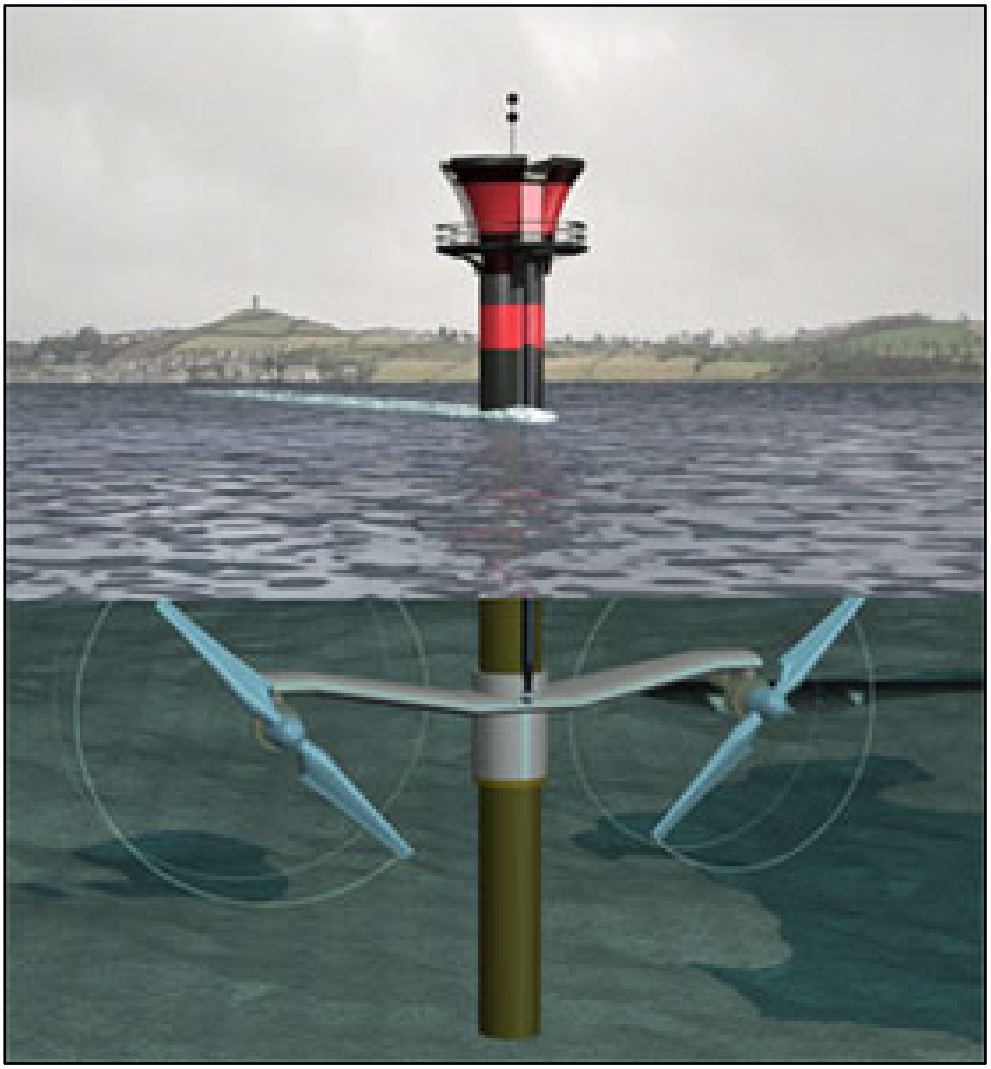

Figure 2 Northern Ireland's Strangford Lough (From [5])

A similar design is the three-bladed turbine produced by Atlantis Resources that is being installed on India's west coast. It will be Asia's first tidal turbine and its three-bladed design will be installed as a turbine farm and expected to produce over 200 Megawatts after development is complete [6].

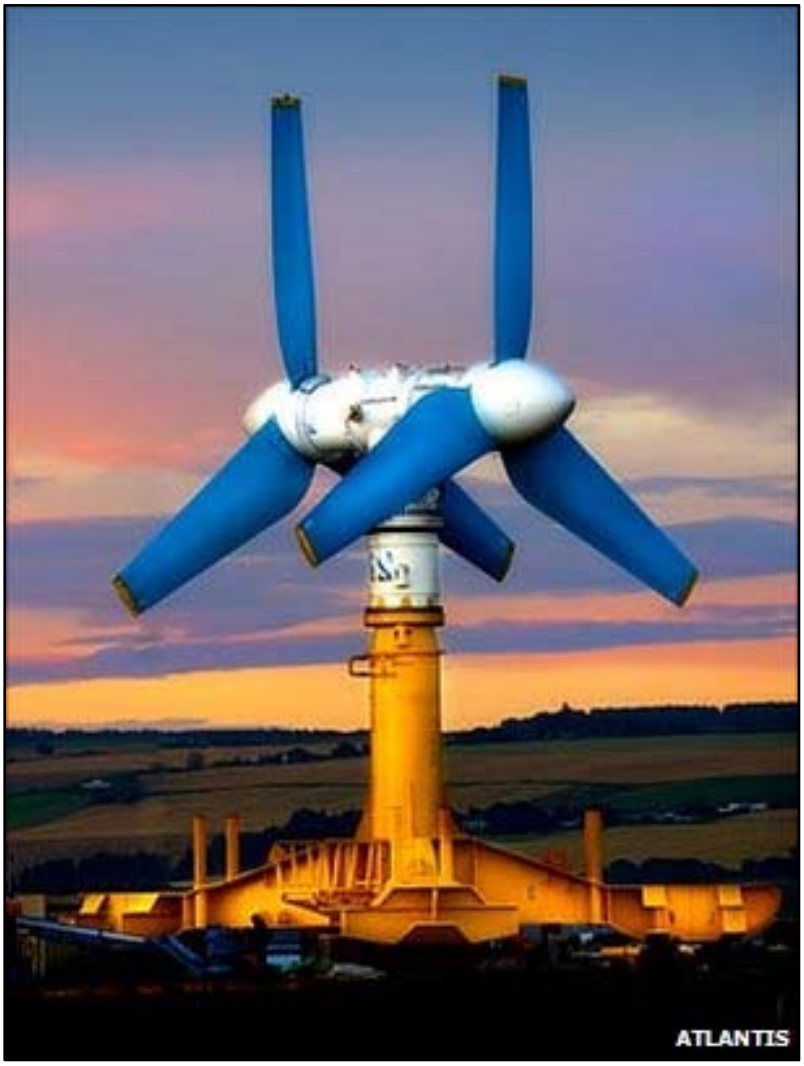


Figure 3 Atlantis AK1000 going to the Gulf of Kutch, India (From [6])

A ducted propeller design has been in production by Lunar Energy [7]. The company is installing a 300 turbine field in South Korea that will become the world's largest tidal turbine installation. Each unit is designed to produce one Megawatt of power, is 11.5 meters wide, and weighs over 2,500 tons. The design is bi-directional which will not require mechanical realignment when the tide shifts. This design feature is a significant power savings and maintenance advantage.

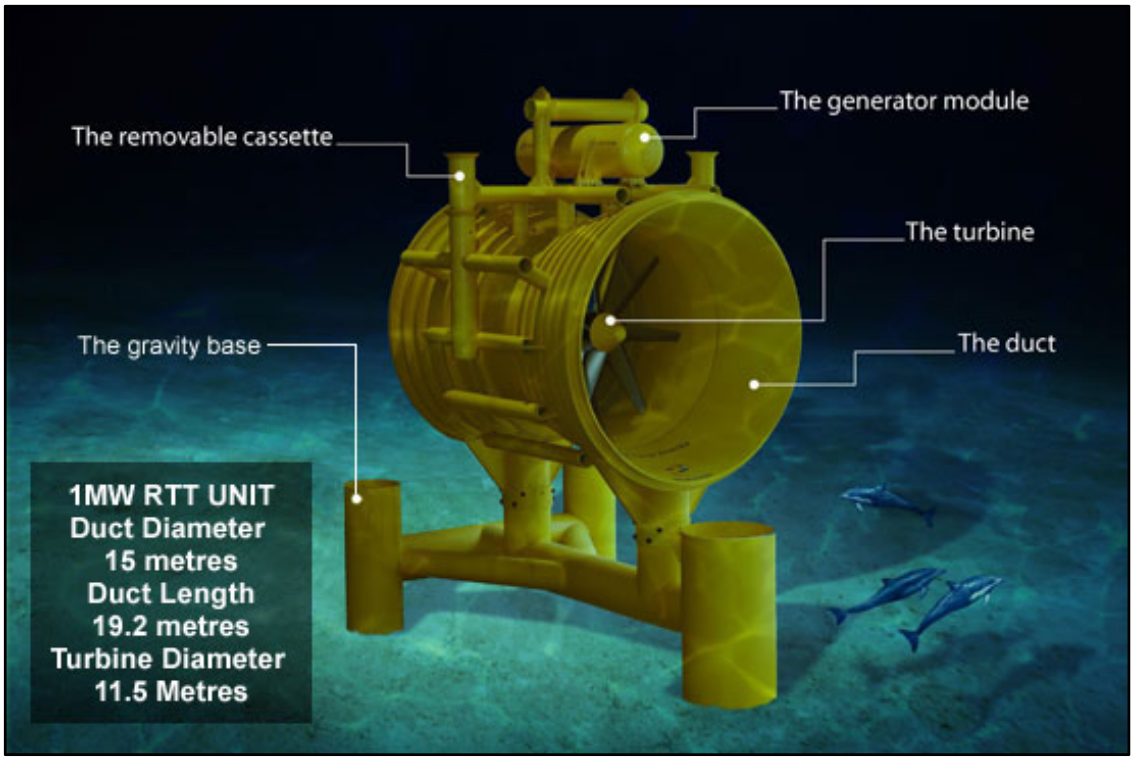


Figure 4 Lunar Energy in Wando Hoenggan Water Way, South Korea (From [7])

One of the newest designs is a vertical axis turbine instead of the traditional horizontal axis design. This design is not bi-directional, but instead uses a pivot system to align it in the proper direction. This Tidal Energy Pty Ltd company's design is one of the most creative designs on the market as it does not rely on currently accepted design configurations.

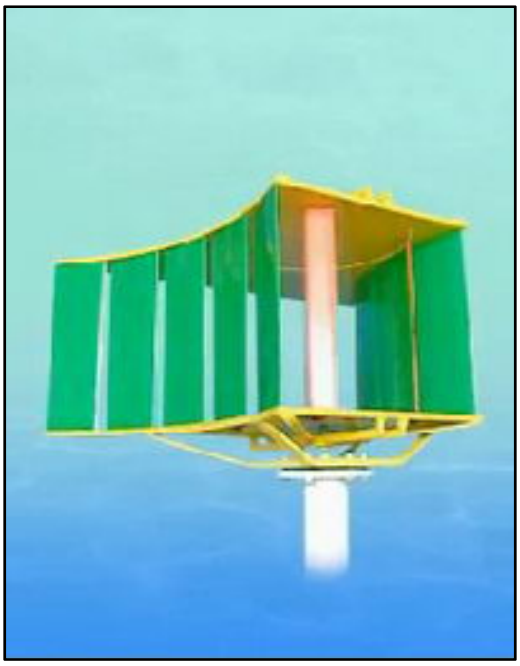

Figure 5 Tidal Energy Pty Ltd supplied to Latin Power Group (From [8])

After analysis of the current designs in the market and research of alternatives to the currently accepted design shapes, a new idea was formed by using a cross-flow tidal turbine with ducting. The design was created so that it can be used in a bi-directional flow arrangement which eliminated the need for mechanical realignment between tidal streams.

The objective of this study was a design to have been suitable for multiple installment locations and tidal current speeds. Hence, a bi-directional design was conceptualized and analyzed at different rotational speeds to determine the highest efficiency for the given scenario. Once efficiency results were established, a further analysis of the number of blades in the rotor were computed to determine the maximum efficiency possible at a given inlet pressure for the system.

# II. PROBLEM DEFINITION

The foundation for the project was outlined by a study completed at Clemson University [3] looking at cross-flow turbine efficiency in a cascade flow design. In the study, the optimum efficiency was found for a cross-flow fan design in terms of number of blades, flow entry angle, and diameter ratio based on blade chord length. The overall design was only based on the Clemson study because changing the flow direction from a cascading gravity fed mono-directional turbine to the bi-directional vertical axis design is significant. The experimental data in the Clemson study was not applicable to this study because of those key differences. The baseline and efficiency principles still applied, but the data was not comparable for this case given the nature of a turbine that can utilize bi-directional flow.

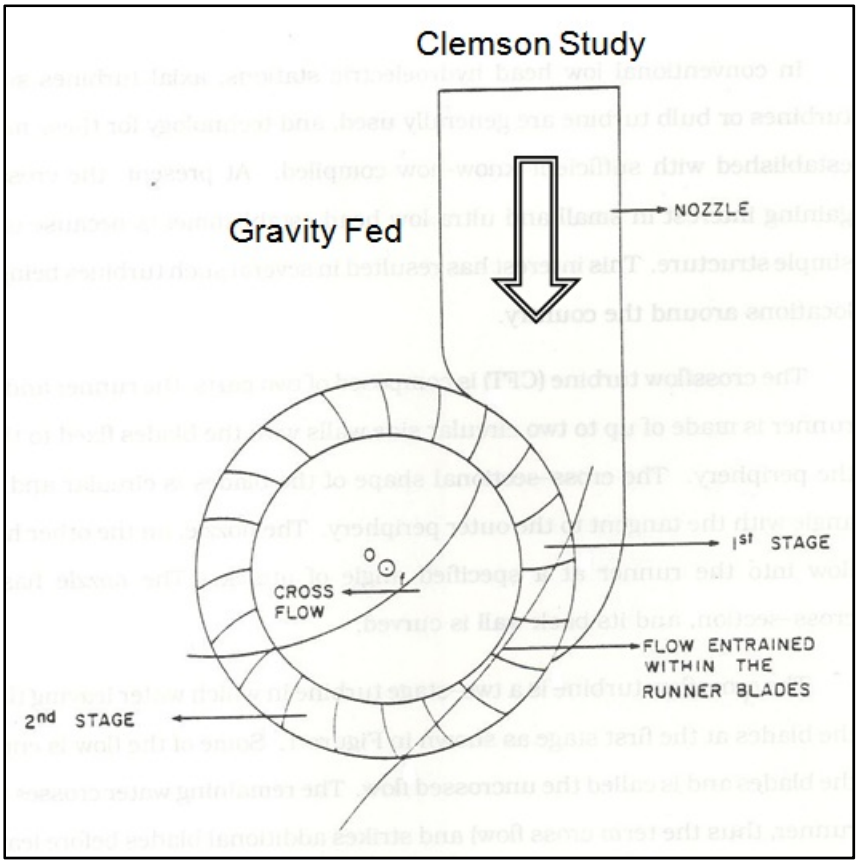


Figure 6 Clemson study of cascading Cross-Flow Turbine (From [3])

THIS PAGE INTENTIONALLY LEFT BLANK

# III. TURBINE DESIGN AND MODELING

## A. GEOMETRY CONCEPTUALIZATION

The design created for this project was based on the specifications provided by the Clemson paper [3] before adjustments were made in consideration of the flow. The shape of the outer wall was designed to be similar to the Clemson inlet shape. The inner wall shape was determined computationally by trial and error. The flow inlet and outlet designs were created anti-symmetrically in order to utilize bi-directional flow. The inlet shape was designed to be larger than the rotor area in order to direct the most water possible through the turbine. The inlet and outlet areas had to be of equal in size and shape. This was done to determine the best inlet size and flow shape to achieve maximum fluid momentum while not sacrificing efficiency when the tide shifts. By creating the anti-symmetrical design, the blades always rotate the same direction which is essential to efficient power production at the generator. The anti-symmetrical design and the rotational direction of the blades as fluid passed through the system is shown in Figure 7.

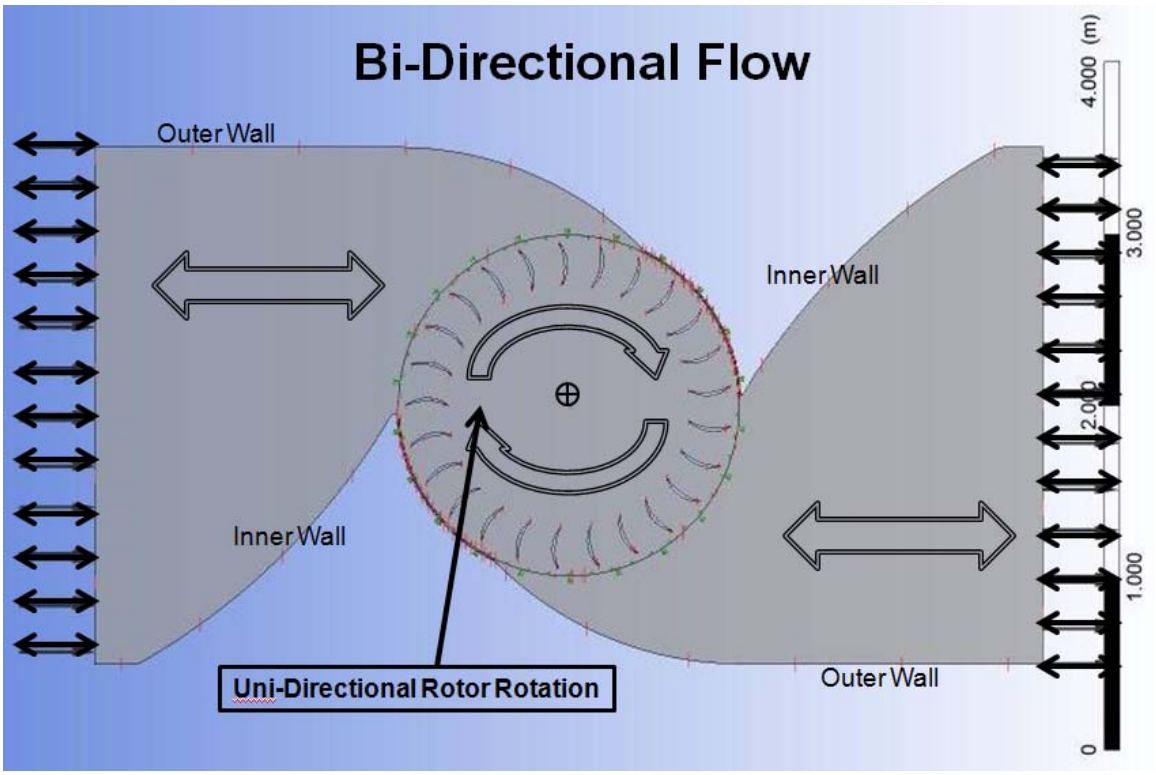


Figure 7 Bi-Directional cross-flow tidal turbine

The rotor design was based on that of the Clemson study [3]. The gravity fed design that was analyzed by Clemson achieved a maximum efficiency with a 25 blade rotor. This 25 blade design was the bases for the rotor. Two of the most influential points of the design were the sharp angles at the point of fluid entry into the rotor from the envelope. The key was to start the opening exactly in-line with the centroid of the rotors to achieve the maximum efficiency.

## B. COMPUTATIONAL FLUIDS MODEL/MESHING

The mesh was produced with the sweep method on proximity and used edge sizing around the blades to ensure the concentration of points on the surfaces of the blades to produce the best resolution possible. The sweep method was setup to sweep both domains together with an All Quad mesh type that utilized a number of divisions of 3 with no bias. During mesh construction, it was important to have enough points across the gap for the sheath going around the rotor domain. This was done by using the

proximity setting for the mesh and setting the points across the gap to five. Without this setting, the simulations failed due to singularities. The relevance center was set to course which was acceptable because the model size made a finer mesh impractical. The minimum size was set to 0.01 mm, maximum face size 0.05 m, and maximum size 0.05 m. Other settings remained in default condition. The mesh settings can be viewed in Figure 19 in Appendix A.

The edge sizing for the blades was imperative so that enough data can be gathered about the behavior of the fluid while flowing over the surface of the blades. The edge sizing for the blade faces used 50 divisions with a bias factor of 30 and a bias shape that put the smaller sizing on the ends of the blades. The blade tips also used edge sizing with 10 divisions and no bias factor. By concentrating data points around the surface of the blades accurate torque data was computed for the turbine.

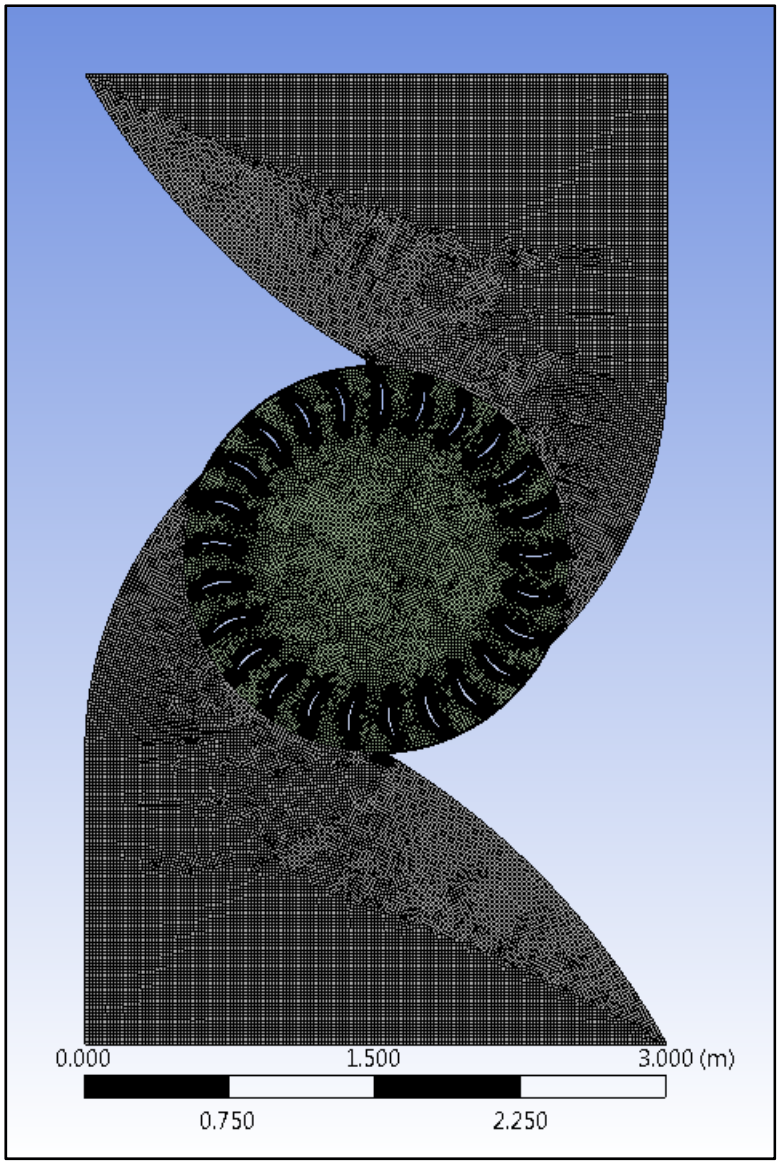


Figure 8 Full mesh

| | Rotor | Envelope |
|---|---|---|
| Nodes | 185624 | 141712 |
| Elements | 134787 | 101223 |

Table 1. Mesh statistics

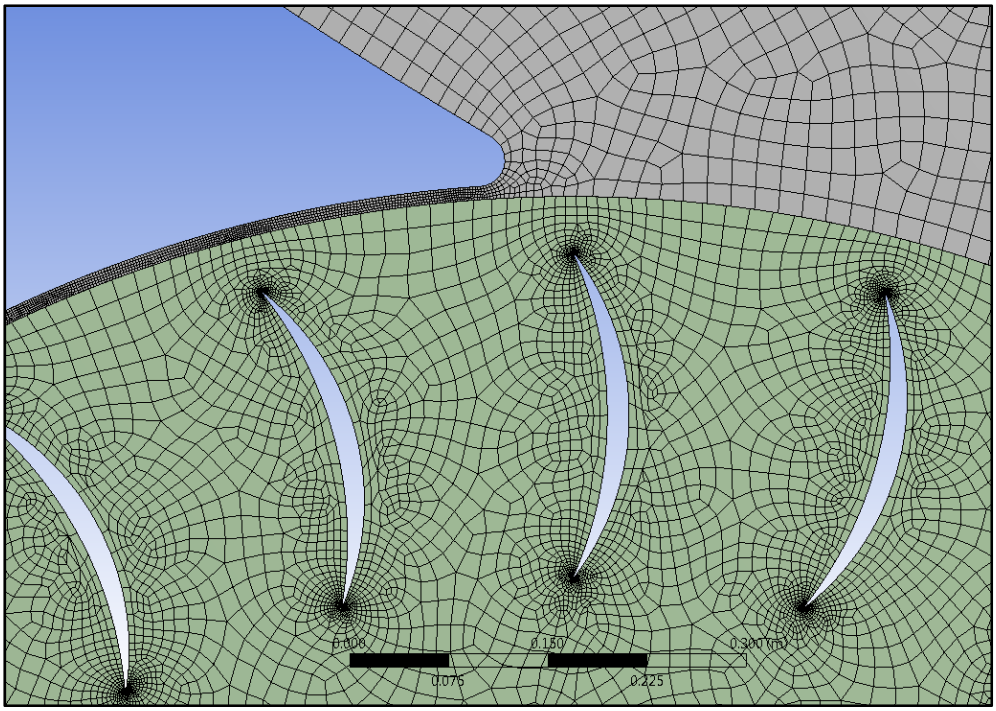


Figure 9 Close up of blade tips and envelope sheath

## C. PROBLEM SPECIFICATIONS AND BOUNDARY CONDITIONS

The simulation definition was created using ANSYS CFX-Pre. The best measurements to determine the efficiency of the system were torque and the change in pressure between the inlet and outlet. The Total Energy fluid model was selected because energy was generated within the turbine control volume. For the purposes of this study, buoyancy and gravity were ignored. An initial velocity condition of 1 meter per second provided a quicker convergence vice starting the flow at a standstill.

Time-step selection was very important to the accuracy of the model. The time-step for the simulations of this study were set to 1 degree of rotation. The Courant number at even slightly larger time-steps increased dramatically and less accurate data was the result. With 1 degree time steps, the Courant number averaged 34.2, which was a reasonable value. An average Courant number below 10 was preferable, but further reduction in time-steps increased simulation time significantly while the 1 degree time step provided sufficiently accurate data.

To have at least one complete rotation of the blades after quasi-equilibrium of the flow field, a total of 1,080 time-steps were calculated with 10 sub-iterations for each time-step. For a speed of 6 revolutions per minute the simulation calculated 30 seconds of real time for a total of 3 full revolutions. Other speeds required different time-step values, but 3 full revolutions were calculated with iterations at 1 degree of rotation regardless of blade speed.

The model was tested at five different blade rotation speeds (1.5, 3, 6, 9, and 12 rpm). Each rotation speed was tested with different inlet gauge pressures from 33 Pascal to 34,000 Pascal. In order to get a complete turbine map, some speeds needed higher or lower inlet pressures to produce the mass flow rate necessary for mapping.

## D. RESULTS AND DISCUSSION

Because the turbine was designed to be used in many locations with variable tidal patterns it was important to test the design under a variety of inlet conditions and rotational speeds. The drop in pressure across the turbine was plotted (Figure 10) against the mass flow rate as a check to ensure that the code predicted the incompressible turbine performance correctly. Other than small variations for different blade speeds the pressure lines were consistent throughout the simulation. The result was confirmed and showed that the data was reasonable for the change in pressure readings.

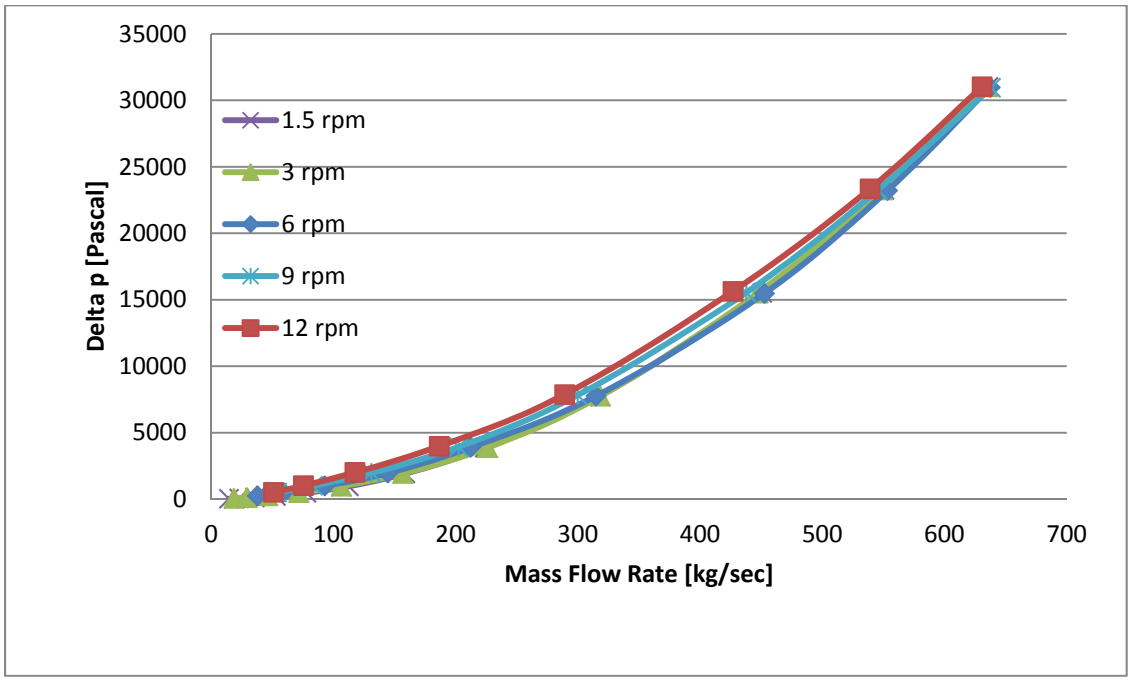


Figure 10 Delta p versus mass flow rate for various turbine rotational speeds

The power produced in the system is determined by the flow rate of water moving through the turbine (Figure 11). The power produced by the bi-directional turbine increases significantly as the mass flow rate increases, but due to the greater losses created by the stronger flow the efficiency actually decreases (Figure 12).

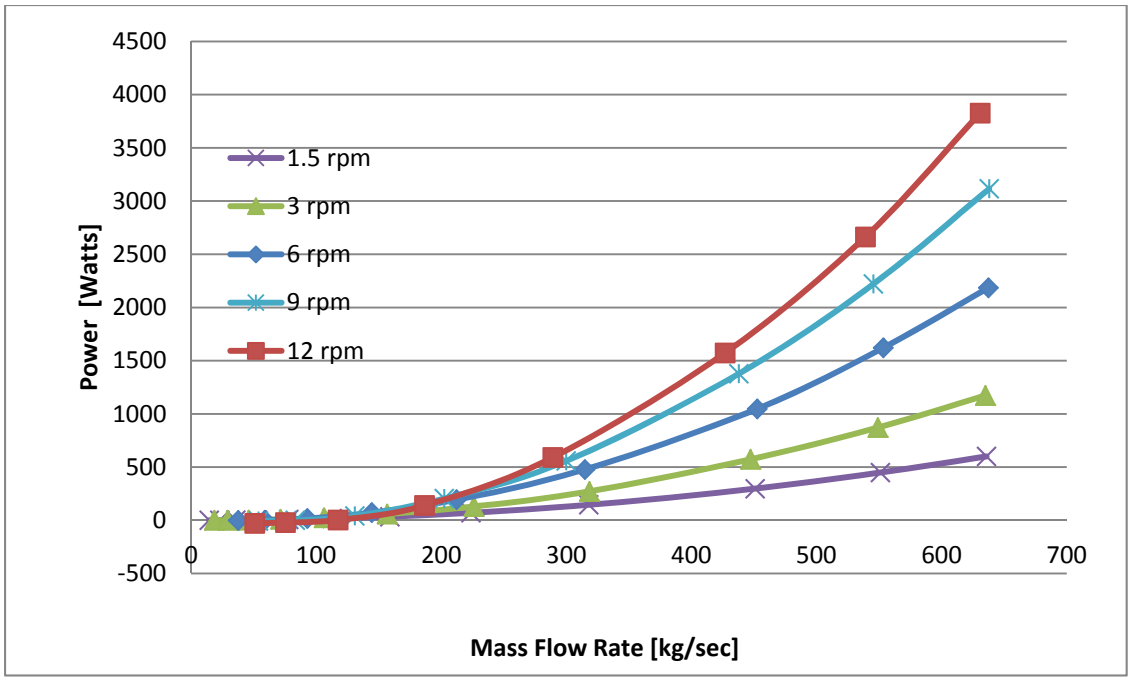


Figure 11 Power versus mass flow rate for various turbine rotational speeds

An efficiency comparison was extremely useful to determine how the turbine would behave in various conditions of fluid flow and provided the key set of data that this study was to determine. The efficiency of the system was determined by monitoring the mass averaged inlet pressure, outlet pressure, and output torque. These were used in the following equations to determine the efficiency of a given set of conditions. Volumetric flow rate was calculated in ANSYS CFX-Post using the expressions calculator.

$$\eta = Power(Actual)/Power(Ideal)$$

$$Power(Actual) = Torque \times \omega$$

$$Power(Ideal) = \Delta p \times Q$$

$$\Delta p = p_{Inlet} - p_{Outlet}$$

$$Q = Volumetric\ Flow\ Rate$$

$$\eta = (Torque \times \omega) \div (\Delta p \times Q)$$

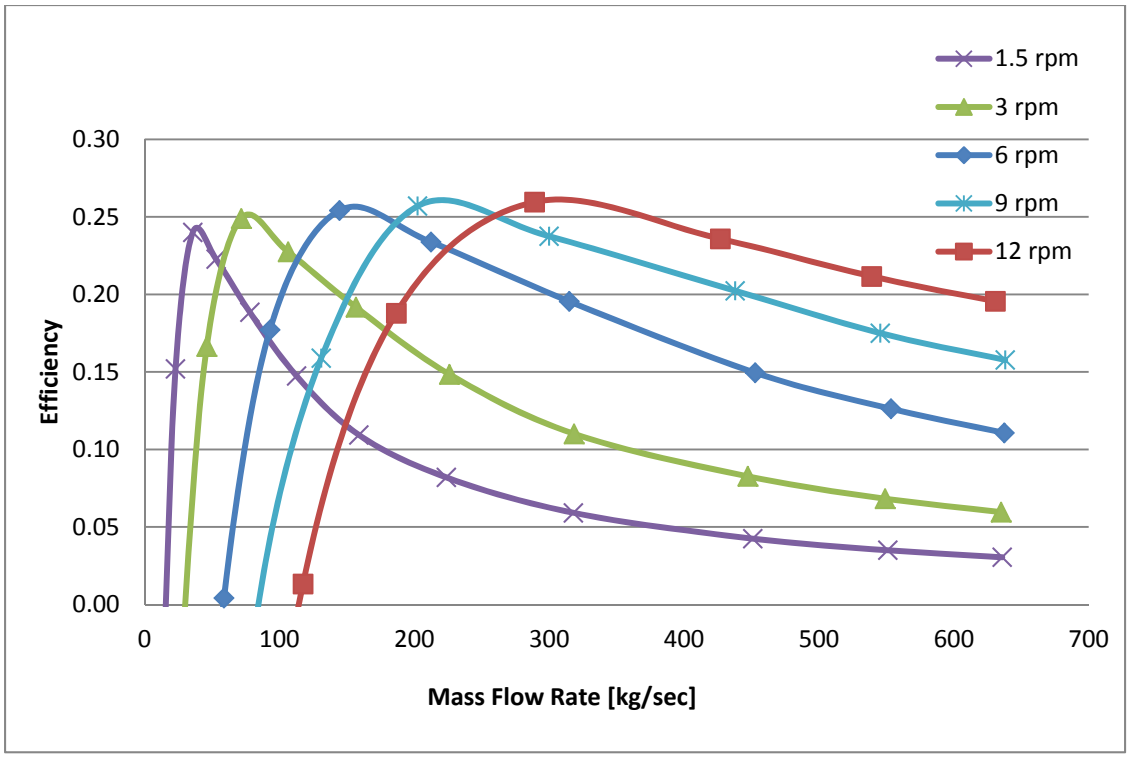


Figure 12 Efficiency versus mass flow rate for various turbine rotational speeds

From the analysis of the data (Figure 12), it was determined that the peak efficiency expected for this design configuration was around 26%. This was compared to the theoretical maximum efficiency for a turbine extracting power from free fluid flow of 59.3% (Ref. [9]). The efficiency for a constant speed peaked at a different mass flow rate, but similar efficiency curves were created as the flow rate changed. Tables in Appendix B show exact data values for the constant speed lines in the above plot.

By analyzing the system further there were several positive and negative flow features for the design. Through the analysis of pressure contours (Figure 13), velocity contour (Figure 14), and velocity vector profiles (Figure 15 and Figure 16) much information was gathered.

First, the pressure contour (Figure 13) was logical as the flow was observed passing from the inlet, through the turbine, and out of the end of the duct. There existed a high pressure region on the concave faces of the blades on the positive torque generating side of the turbine with low pressure regions that existed on the back side of the blades. However, on the negative torque side of the rotor high pressure existed on the back of the blades with low pressure on the concave surfaces.

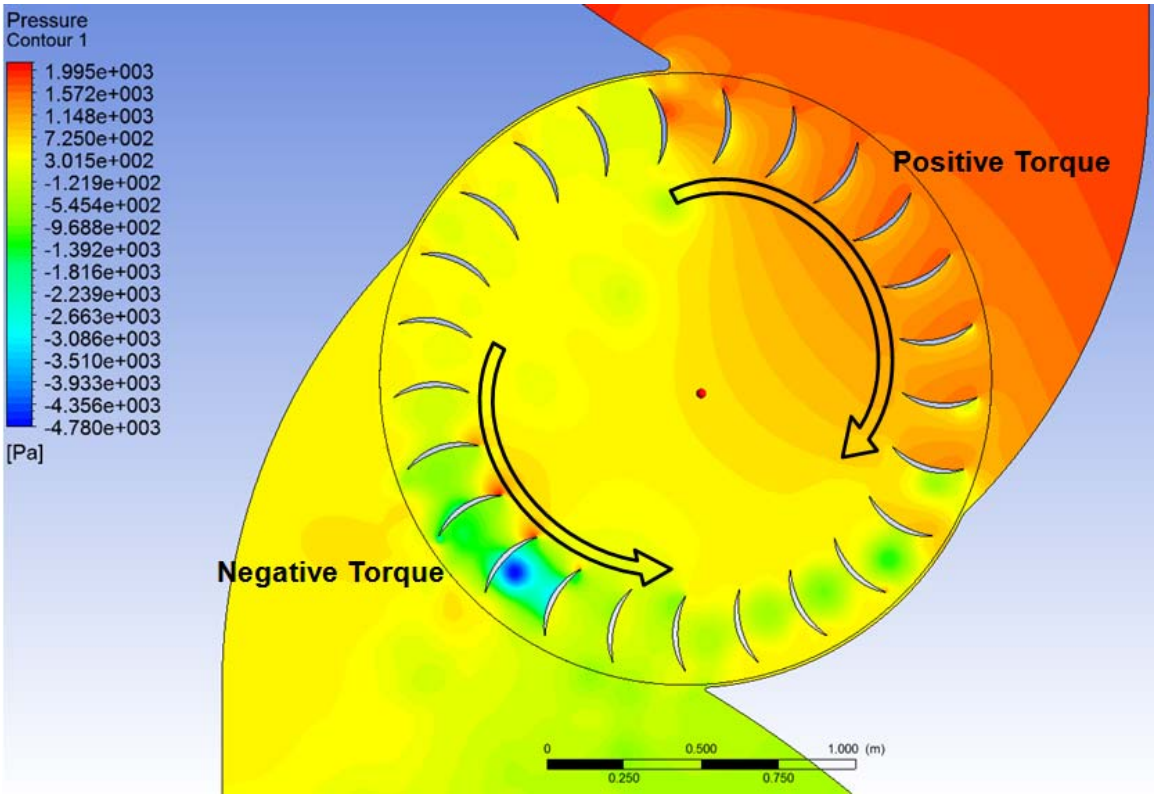


Figure 13 Pressure contours for 6 rpm and inlet pressure of 2125 Pa

The velocity contour plot (Figure 14) provided a snapshot of fluid activity and local areas of significance. When the fluid first enters the rotor, the transition of the first blade from a negative torque producing blade to a positive torque producing blade was clear. The vortices created when the blades passed through the sheathed section of the envelope created negative torque as the fluid circulated from the concave side of one blade to the convex side of the other. As the fluid exited the rotor, the high velocity regions showed the areas of significant pressure drop.

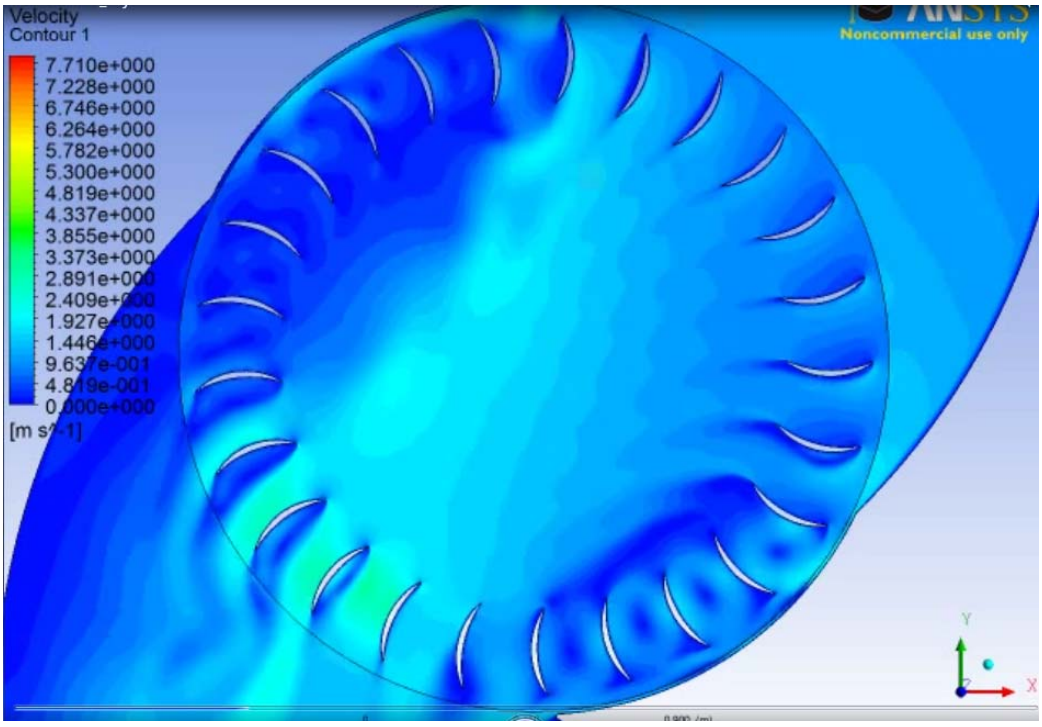


Figure 14 Velocity contours for 6 rpm at inlet pressure 2125 Pa

The flow at the very top of the entrance area and the area at the exit were interesting because they affect much of the performance. A closer look at each area showed regions of high velocity, this was associated with high total pressure losses.

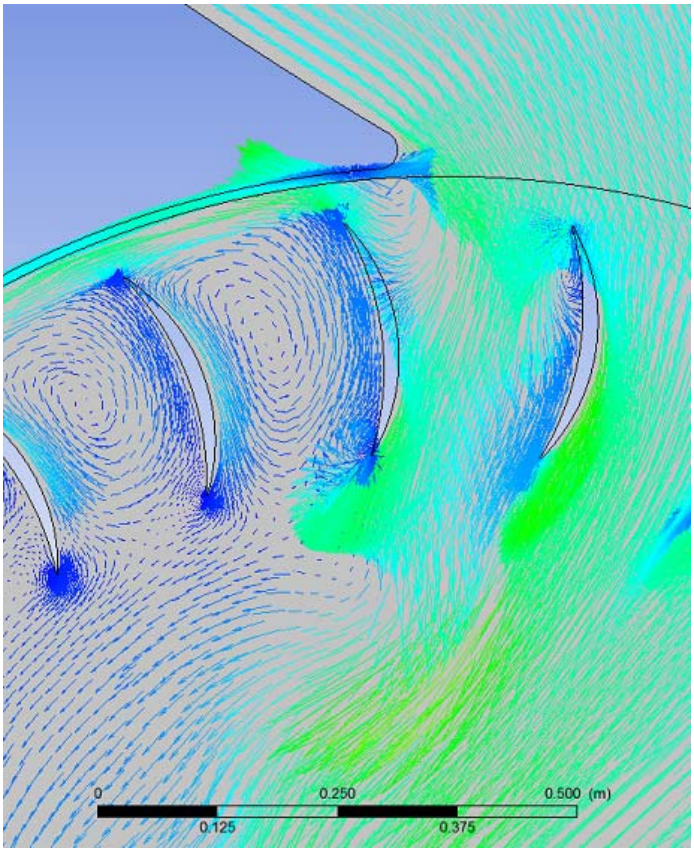


Figure 15 Rotor inlet velocity vector plot for 6 rpm at inlet pressure 2125 Pa

At the point of entry (Figure 15), the fluid was highly active as it interacted with the blades and was entrained outside of the blades and followed the sheath of the envelope. The design of the envelope and the entrance angle of the fluid caused a reverse torque to be created when the fluid wrapped around the entrance and made contact with the blade face. The vortices within the blade gaps also developed a reverse torque on the system and thus reduced the efficiency. A similar situation was also evident as the fluid exited the rotor.

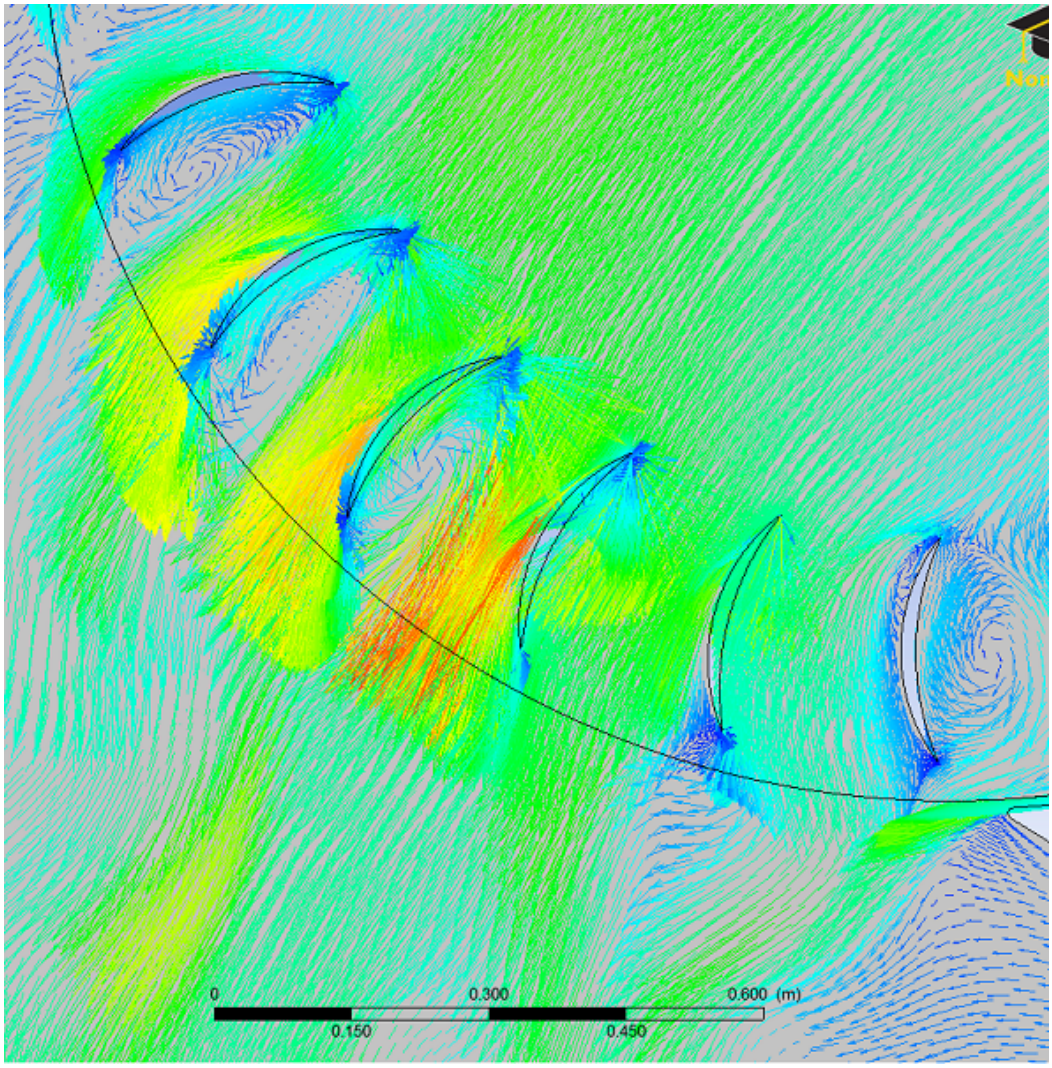


Figure 16 Rotor exit velocity vectors for 6 rpm at inlet pressure 2125 Pa

The flow path of the fluid again reversed the torque on the system causing a reduction in torque and thus power generation as seen in Figure 16.

THIS PAGE INTENTIONALLY LEFT BLANK

# IV. DESIGN IMPROVEMENTS

## A. ROTOR CONFIGURATIONS

Turbine maps were developed for the 25 bladed rotor. The number of blades on the rotor were adjusted to determine the optimum number of blades to produce maximum efficiency. An analysis was conducted of the 9 rpm and 6 rpm blade speeds to determine the best number of blades. Computations were done for 20 and 30 blade configurations in addition to the 25 blade study already completed.

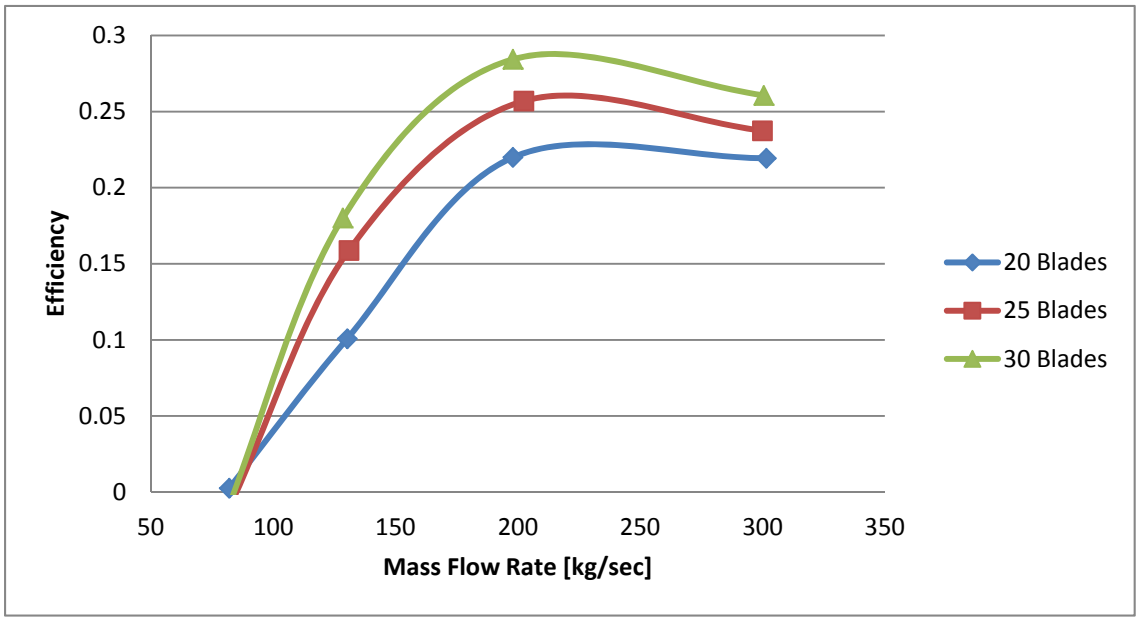


Figure 17 Efficiency versus mass flow rate for various blade numbers at 9 rpm

The initial predictions (Figure 17) showed a clear increase in efficiency for higher blade numbers and hence further analysis was done for the highest efficiency for the 6 revs/min case study in the form of 35, 40, and 45 blades.

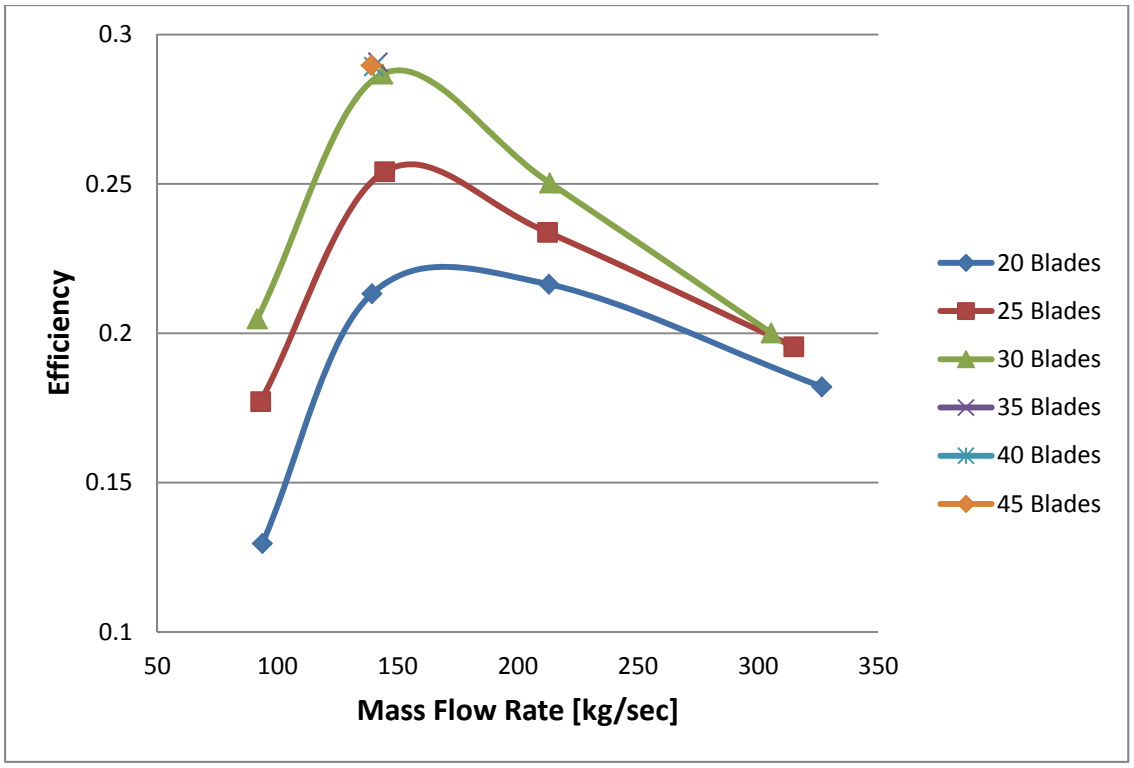


Figure 18 Efficiency versus mass flow rate for various blade numbers at 6 rpm

For the 6 revs/min case study (Figure 18), it was clear that as blade numbers increased the efficiency of the system also increased. Based on the data calculated by CFD, the peak efficiency levels off at 29% for all three new cases of 35, 40, and 45 blades.

## B. ROTOR RECONFIGURATION RESULTS AND DISCUSSION

The information from the study of varying the blade numbers proved that a higher blade count increased efficiency. Theoretically, the efficiency should drop after too many blades are added resulting in excessive blockage. However, up to the 45 blade case, a drop in efficiency had not been predicted (Figure 19) although the efficiency did level off.

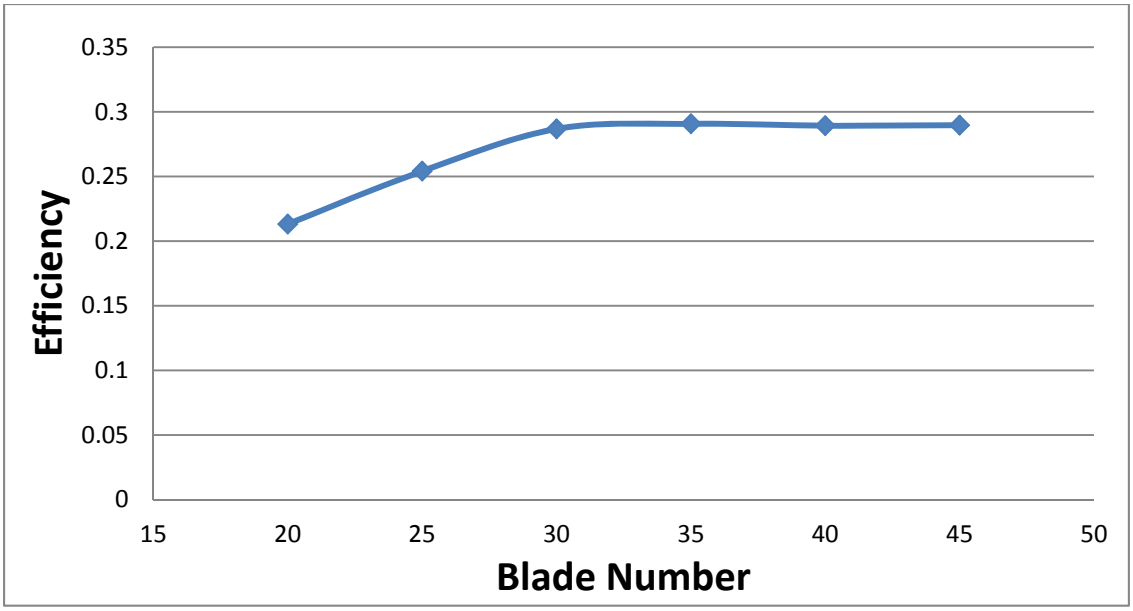


Figure 19 Efficiency versus blade number for 6 rpm

THIS PAGE INTENTIONALLY LEFT BLANK

# V. CONCLUSIONS AND RECOMMENDATIONS

Based on this study, it is possible to use a bi-directional cross-flow turbine to produce rotational power from tidal energy. The efficiency, at which the current design extracts the power at 26%, is low, however when compared to the Betz limit of 59.3% this concept is reasonable. Therefore, the cross-flow tidal turbine technology is feasible, but a much higher efficiency is required before the system would be economically viable for large production.

The optimum blade number is not calculated specifically, but will be found between thirty and forty blades. This is based on the additional study of 6 rpm as forty-five blades shows no improvement for efficiency when compared to the lower blade numbers.

Three future design changes should be considered to improve the efficiency of the system based on this study. The design changes for future studies are the entry and exit point of the flow going through the rotor domain, the length and shape of the blades, and the outside wall angle as the fluid is ducted into the blades.

The entry point of flow at the entrance and exit of the rotor area can be shifted further around the circle in the clockwise direction which will direct more flow on the blade surface. This would increase flow speed while simultaneously producing a better angle of attack on the blades as they pass through the flow field. Future designs altering this entry and exit point should be able to find the most efficient placement for the turbine as well as the entry angle that is most beneficial.

The blade shape is a major factor on torque production by the fluid flow. The increase or decrease of the radius of curvature of the blades will significantly impact the efficiency that a given flow condition can produce with the turbine. As the flow passes through the blades, the first pass is on the concave side of the blade providing max torque for the turbine; however, the second pass is on the convex side of the blade which produces an opposing torque in the reverse direction. There are many standard blade shapes which can be considered and will be researched prior to future iterations along

with unique configurations which may be more effective. One idea is to flatten the blade. This would mostly eliminate the negative torque on the blades as the fluid flow exits. It would also reduce eddies and vortices while providing a flat face for the fluid flow to produce positive torque while entering the turbine. The high velocity zone at the exit will have a reduced effect with its producing of a local low pressure zone

A third design change is the lowest section of the inlet duct. If the wall were to have a more sloped design, the angle of the flow field is altered to a more optimal attack angle on the blades. This will produce more consistent torque production as the blades travel through the power section and will increase efficiency. There is no foreseeable negative impact to adjusting this part of the design as it is inconsequential to the downstream portion of the turbine.

Other changes for future studies can involve the mesh resolution. By refining the mesh, a more accurate picture inside the turbine will be produced. First, adding inflation layers on the blade surfaces will show more detailed boundary layer development. Second, a finer mesh around the contact point between the domains will provide a more accurate depiction of the fluid behavior as it transitions from envelope to rotor domains.

# APPENDIX A. MESH SETUP

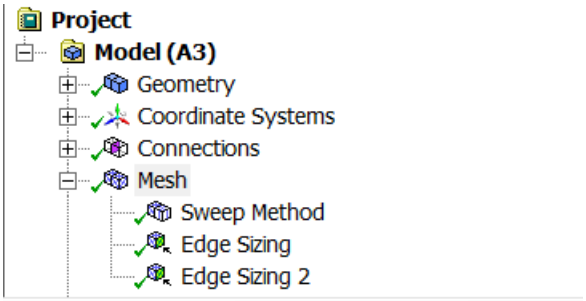


Details of "Mesh"

| | |
|---|---|
| **Defaults** | |
| Physics Preference | CFD |
| Solver Preference | CFX |
| Relevance | 0 |
| **Sizing** | |
| Use Advanced Siz... | On: Proximity |
| Relevance Center | Coarse |
| Initial Size Seed | Active Assembly |
| Smoothing | Medium |
| Transition | Slow |
| Span Angle Center | Fine |
| Proximity Accu... | 0.5 |
| Num Cells Acr... | 5 |
| Min Size | 1.e-005 m |
| Max Face Size | 5.e-002 m |
| Max Size | 5.e-002 m |
| Growth Rate | Default (1.20 ) |
| Minimum Edge L... | 1.4516e-003 m |
| **Inflation** | |
| **Advanced** | |
| **Defeaturing** | |
| **Statistics** | |
| Nodes | 327336 |
| Elements | 236010 |
| Mesh Metric | None |

Figure 20 Full mesh setup and sizing

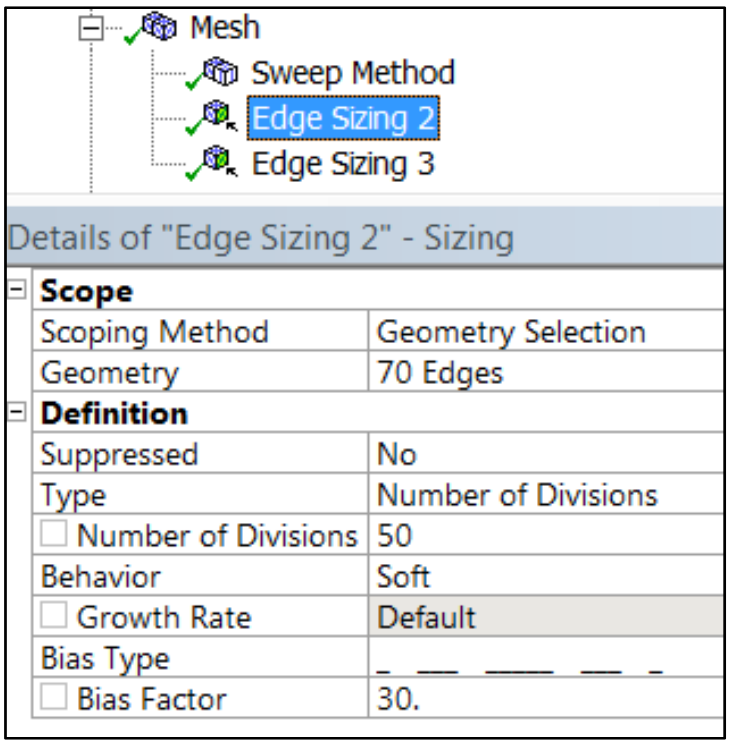


Figure 21 Blade faces mesh setup and sizing

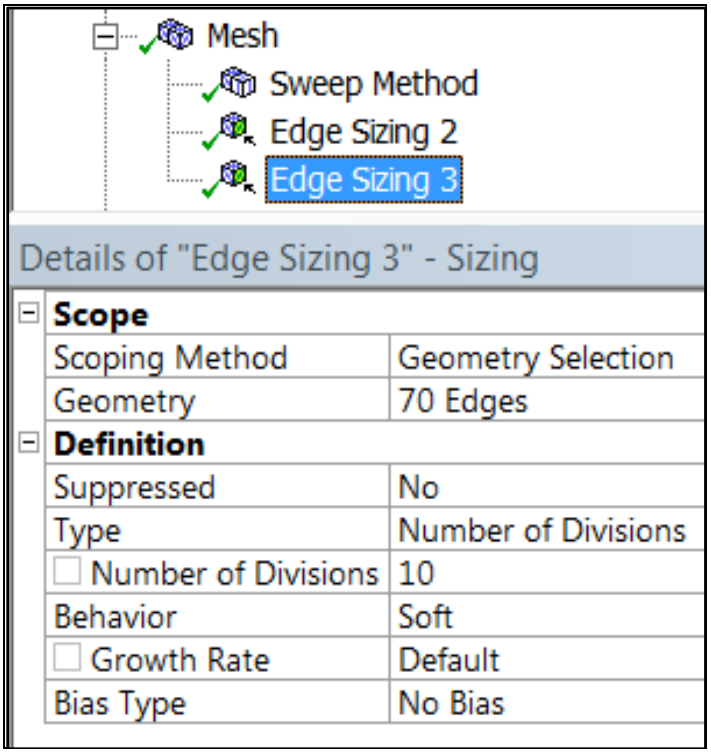


Figure 22 Blade tips mesh setup and sizing

# APPENDIX B. RESULTS TABLES FOR 25 BLADE ROTOR

| 1.5 rpm | | | | | |
|---|---|---|---|---|---|
| Inlet Pressure [Pascal] | Mass Flow Rate [kg/s] | Delta p [Pascal] | Calc. Eff. | Torque [N*m] | Power [W] |
| 33 | 14.520 | 31.348 | -0.028 | -0.080 | -0.013 |
| 66.25 | 22.886 | 62.289 | 0.152 | 1.378 | 0.217 |
| 132.5 | 35.678 | 122.958 | 0.240 | 6.700 | 1.052 |
| 265 | 52.993 | 244.281 | 0.223 | 18.355 | 2.883 |
| 531.25 | 78.021 | 485.965 | 0.189 | 45.503 | 7.148 |
| 1062.5 | 112.717 | 967.885 | 0.147 | 102.346 | 16.076 |
| 2125 | 158.873 | 1936.756 | 0.109 | 214.172 | 33.642 |
| 4250 | 223.749 | 3876.024 | 0.082 | 452.652 | 71.102 |
| 8500 | 317.908 | 7754.081 | 0.059 | 927.333 | 145.665 |
| 17000 | 450.916 | 15506.567 | 0.042 | 1891.060 | 297.047 |
| 25500 | 551.046 | 23258.099 | 0.035 | 2855.810 | 448.590 |
| 34000 | 635.906 | 31009.740 | 0.030 | 3822.017 | 600.361 |

| 3 rpm | | | | | |
|---|---|---|---|---|---|
| Inlet Pressure [Pascal] | Mass Flow Rate [kg/s] | Delta p [Pascal] | Calc. Eff. | Torque [N*m] | Power [W] |
| 66.25 | 18.533 | 63.281 | -0.202 | -0.755 | -0.237 |
| 132.5 | 29.159 | 125.790 | -0.013 | -0.148 | -0.047 |
| 265 | 46.044 | 248.859 | 0.166 | 6.068 | 1.906 |
| 531.25 | 71.588 | 492.418 | 0.249 | 27.934 | 8.776 |
| 1062.5 | 106.343 | 978.087 | 0.227 | 75.314 | 23.661 |
| 2125 | 156.707 | 1941.759 | 0.192 | 185.699 | 58.339 |
| 4250 | 226.006 | 3870.408 | 0.148 | 413.309 | 129.845 |
| 8500 | 318.403 | 7745.212 | 0.110 | 863.460 | 271.264 |
| 17000 | 447.239 | 15500.460 | 0.083 | 1823.882 | 572.989 |
| 25500 | 549.036 | 23256.115 | 0.068 | 2774.352 | 871.588 |
| 34000 | 635.050 | 31007.892 | 0.060 | 3735.409 | 1173.513 |

| 6 rpm | | | | | |
|---|---|---|---|---|---|
| Inlet Pressure [Pascal] | Mass Flow Rate [kg/s] | Delta p [Pascal] | Calc. Eff. | Torque [N*m] | Power [W] |
| 265 | 37.706 | 253.496 | -0.216 | -3.291 | -2.068 |
| 531.25 | 58.854 | 504.705 | 0.004 | 0.196 | 0.123 |
| 1062.5 | 92.934 | 996.935 | 0.177 | 26.123 | 16.413 |
| 2125 | 144.499 | 1967.663 | 0.254 | 114.988 | 72.249 |
| 4250 | 212.284 | 3908.935 | 0.234 | 308.768 | 194.005 |
| 8500 | 314.789 | 7756.228 | 0.196 | 759.788 | 477.389 |
| 17000 | 452.642 | 15477.148 | 0.149 | 1666.580 | 1047.143 |
| 25500 | 553.414 | 23215.163 | 0.126 | 2581.270 | 1621.860 |
| 34000 | 637.396 | 30972.619 | 0.111 | 3477.561 | 2185.016 |

| 9 rpm | | | | | |
|---|---|---|---|---|---|
| Inlet Pressure [Pascal] | Mass Flow Rate [kg/s] | Delta p [Pascal] | Calc. Eff. | Torque [N*m] | Power [W] |
| 531.25 | 53.956 | 507.053 | -0.266 | -7.722 | -7.278 |
| 1062.5 | 83.360 | 1009.006 | -0.006 | -0.498 | -0.470 |
| 2125 | 130.917 | 1994.701 | 0.159 | 44.004 | 41.473 |
| 4250 | 202.425 | 3938.887 | 0.257 | 217.383 | 204.879 |
| 8500 | 299.936 | 7826.772 | 0.237 | 591.444 | 557.423 |
| 17000 | 437.866 | 15543.353 | 0.202 | 1461.173 | 1377.124 |
| 25500 | 545.478 | 23262.571 | 0.175 | 2355.950 | 2220.431 |
| 34000 | 638.065 | 30954.982 | 0.158 | 3305.481 | 3115.342 |

| 12 rpm | | | | | |
|---|---|---|---|---|---|
| Inlet Pressure [Pascal] | Mass Flow Rate [kg/s] | Delta p [Pascal] | Calc. Eff. | Torque [N*m] | Power [W] |
| 531.25 | 50.868 | 511.200 | -1.076 | -22.274 | -27.990 |
| 1062.5 | 75.399 | 1018.029 | -0.274 | -16.746 | -21.044 |
| 2125 | 117.445 | 2020.347 | 0.013 | 2.508 | 3.151 |
| 4250 | 186.538 | 3984.848 | 0.188 | 111.145 | 139.669 |
| 8500 | 289.078 | 7868.043 | 0.260 | 469.876 | 590.463 |
| 17000 | 426.869 | 15627.935 | 0.236 | 1251.778 | 1573.030 |
| 25500 | 539.048 | 23345.693 | 0.212 | 2119.120 | 2662.964 |
| 34000 | 630.775 | 31026.065 | 0.196 | 3045.486 | 3827.071 |

# APPENDIX C. VARIABLE BLADE RESULTS FOR 6 RPM SPEED

| **20 Blades** | | | | |
|---|---|---|---|---|
| Inlet Pressure [Pascal] | Mass Flow Rate [kg/sec] | Delta p [Pascal] | Torque (N*m) | Calc. Eff. |
| 1062.5 | 93.677 | 995.931 | 19.247 | 0.130 |
| 2125 | 139.286 | 1976.812 | 93.452 | 0.213 |
| 4250 | 212.911 | 3907.888 | 286.581 | 0.216 |
| 8500 | 326.477 | 7713.458 | 729.789 | 0.182 |
| **25 Blades** | | | | |
| Inlet Pressure [Pascal] | Mass Flow Rate [kg/sec] | Delta p [Pascal] | Torque (N*m) | Calc. Eff. |
| 1062.5 | 92.934 | 996.935 | 26.123 | 0.177 |
| 2125 | 144.499 | 1967.663 | 114.988 | 0.254 |
| 4250 | 212.284 | 3908.935 | 308.768 | 0.234 |
| 8500 | 314.789 | 7756.228 | 759.788 | 0.196 |
| **30 Blades** | | | | |
| Inlet Pressure [Pascal] | Mass Flow Rate [kg/sec] | Delta p [Pascal] | Torque (N*m) | Calc. Eff. |
| 1062.5 | 91.488 | 998.637 | 29.785 | 0.205 |
| 2125 | 143.661 | 1968.994 | 129.120 | 0.287 |
| 4250 | 213.217 | 3911.005 | 332.242 | 0.250 |
| 8500 | 305.369 | 7800.779 | 758.748 | 0.200 |
| **35 Blades** | | | | |
| Inlet Pressure [Pascal] | Mass Flow Rate [kg/sec] | Delta p [Pascal] | Torque (N*m) | Calc. Eff. |
| 2125 | 141.742 | 1973.176 | 129.420 | 0.291 |
| **40 Blades** | | | | |
| Inlet Pressure [Pascal] | Mass Flow Rate [kg/sec] | Delta p [Pascal] | Torque (N*m) | Calc. Eff. |
| 2125 | 139.979 | 1977.124 | 127.433 | 0.289 |
| **45 Blades** | | | | |
| Inlet Pressure [Pascal] | Mass Flow Rate [kg/sec] | Delta p [Pascal] | Torque (N*m) | Calc. Eff. |
| 2125 | 139.286 | 1979.348 | 126.781 | 0.289 |

THIS PAGE INTENTIONALLY LEFT BLANK

# APPENDIX D. VARIABLE BLADE RESULTS FOR 9 RPM SPEED

| **20 Blades** | | | | |
|---|---|---|---|---|
| Inlet Pressure [Pascal] | Mass Flow Rate [kg/sec] | Delta p [Pascal] | Torque (N*m) | Calc. Eff. |
| 1062.5 | 82.014 | 1010.200 | 0.227 | 0.003 |
| 2125 | 130.268 | 1995.067 | 27.793 | 0.101 |
| 4250 | 197.982 | 3955.275 | 182.737 | 0.220 |
| 8500 | 301.591 | 7819.617 | 548.801 | 0.219 |
| **25 Blades** | | | | |
| Inlet Pressure [Pascal] | Mass Flow Rate [kg/sec] | Delta p [Pascal] | Torque (N*m) | Calc. Eff. |
| 1062.5 | 83.360 | 1009.006 | -0.498 | -0.006 |
| 2125 | 130.917 | 1994.701 | 44.004 | 0.159 |
| 4250 | 202.425 | 3938.887 | 217.383 | 0.257 |
| 8500 | 299.936 | 7826.772 | 591.444 | 0.237 |
| **30 Blades** | | | | |
| Inlet Pressure [Pascal] | Mass Flow Rate [kg/sec] | Delta p [Pascal] | Torque (N*m) | Calc. Eff. |
| 1062.5 | 79.704 | 1014.007 | -1.558 | -0.018 |
| 2125 | 128.436 | 1999.510 | 49.071 | 0.180 |
| 4250 | 197.982 | 3946.265 | 239.267 | 0.284 |
| 8500 | 300.465 | 7826.774 | 650.477 | 0.261 |

THIS PAGE INTENTIONALLY LEFT BLANK

# APPENDIX E. ENVELOPE GEOMETRY GENERATION

A. Launch **SolidWorks 2010**.

1. In the **SolidWorks** Banner, Select **File > New Project** from the Main Menu and click on **Part – a 3D representation of a single design component > OK.**
2. In the **SolidWorks** Banner, Select **Tools > Options > Document Properties – Units.** Ensure that **MKS (meter, kilogram, second)** is selected.

B. Draw 2D Envelope.

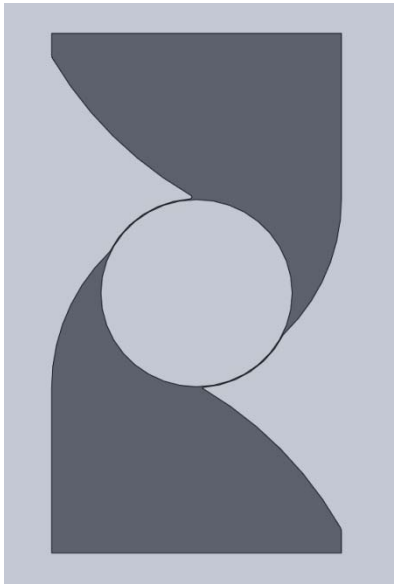

Figure 23 Envelope design

1. Point Creation.
   a. Click on the blue **Z-Plane** arrow in the bottom left of the window.
   b. Right click on the **Front Plane** in the design tree on the left side of the window and choose the **Sketch** feature.

c. Click on the **Point** feature to sketch a point. The bold locations in the table are to be fixed. This is done by clicking the **Fix** icon while inputting the points.

| Point | X Parameter | Y Parameter |
|---|---|---|
| **1** | **-1.5** | **-1** |
| **2** | **-1.5** | **-2.75** |
| **3** | **1.5** | **-2.75** |
| 4 | 1.5 | -2.5 |
| 5 | 0 | -1 |
| 6 | 0.9 | -0.45 |
| **7** | **1.5** | **1** |
| **8** | **1.5** | **2.75** |
| **9** | **-1.5** | **2.75** |
| 10 | -1.5 | 2.5 |
| 11 | 0 | 1 |
| 12 | -0.9 | 0.45 |

Table 2. Envelope sketch points

2. Draw lines connecting the points.

   a. Connect the following points together with the **Line** feature.

      i. **1 > 2 , 2 > 3 , 3 > 4**

      ii. **7 > 8 , 8 > 9 , 9 > 10**

   b. Connect the following points together with the **Three Point Arc** feature.

      i. **4 > 5 , 5 > 6 , 6 > 7**

      ii. **10 > 11 , 11 > 12 , 12 > 13**

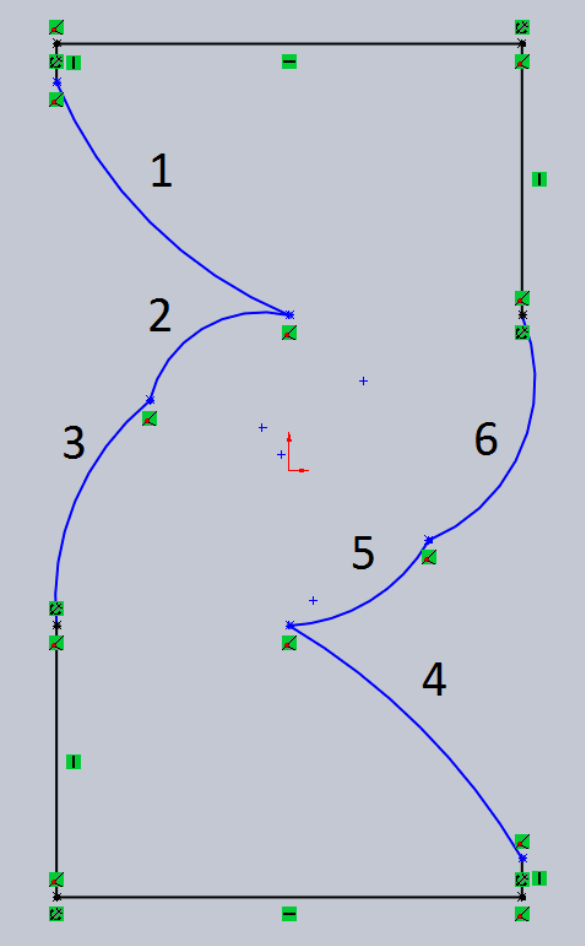


Figure 24 Rough imagine of envelope

3. Correct the shape of each arc by selecting the arc individually and changing the input to look like the Table:

| Curves | Radius (m) |
|---|---|
| 1 | 4 |
| 2 | 1 |
| 3 | 2 |
| 4 | 4 |
| 5 | 1 |
| 6 | 2 |

Table 3. Radius of curvature for envelope walls

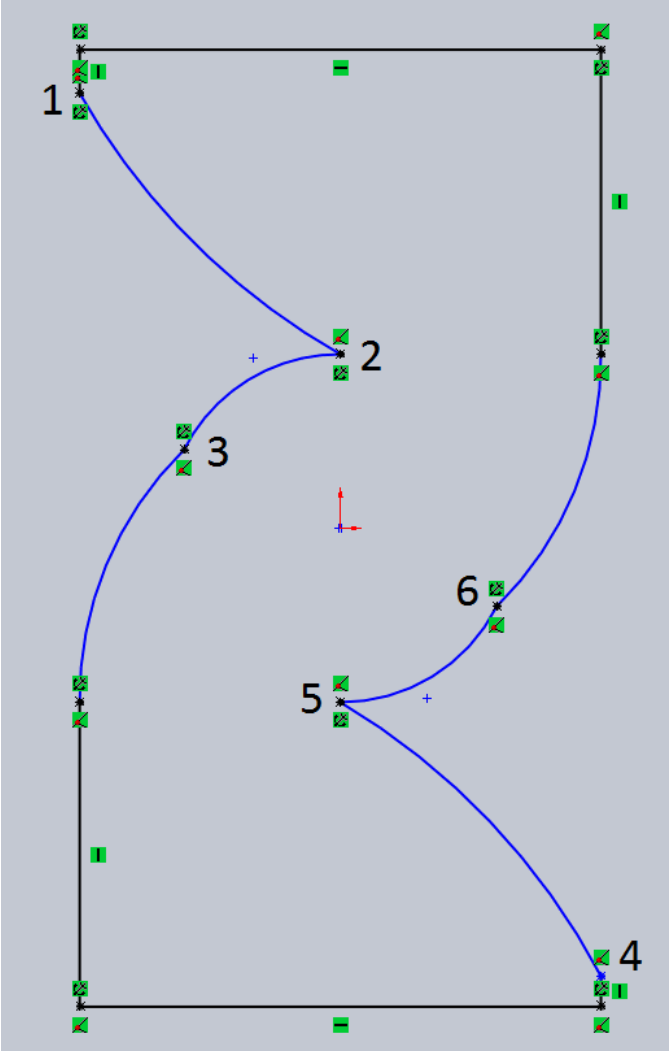


Figure 25 Finished curves before fillets

4. Soften the edges of the curves by adding a **Fillet** at the important junctures.
   a. Click the **Fillet** feature. While holding down the **CTRL** key, select both lines on either side of the connections enumerated above. Once selected, enter the **Fillet Parameters** as listed in the table.

| Fillet | Fillet Parameter (m) |
|---|---|
| 1 | 0.1 |
| 2 | 0.02 |
| 3 | 0.02 |
| 4 | 0.1 |
| 5 | 0.02 |
| 6 | 0.02 |

Table 4. Envelope fillet parameters

Once Fillets have been completed the figure will appear as in the Figure.

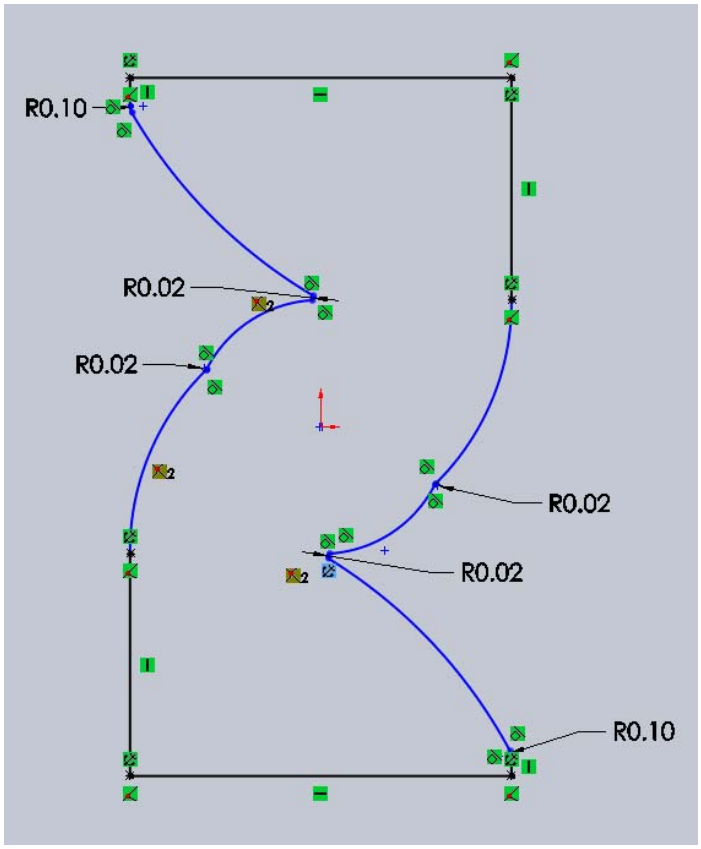


Figure 26 Finished fillets

5. Ensure proper radii of arcs by using the **Smart Dimension** feature. Use the feature on the two shortest segments of arc to ensure a Radii equal to 1m. Next, make sure there is a 0.45m distance between the origin and each fillet centroid as it appears in the figure.

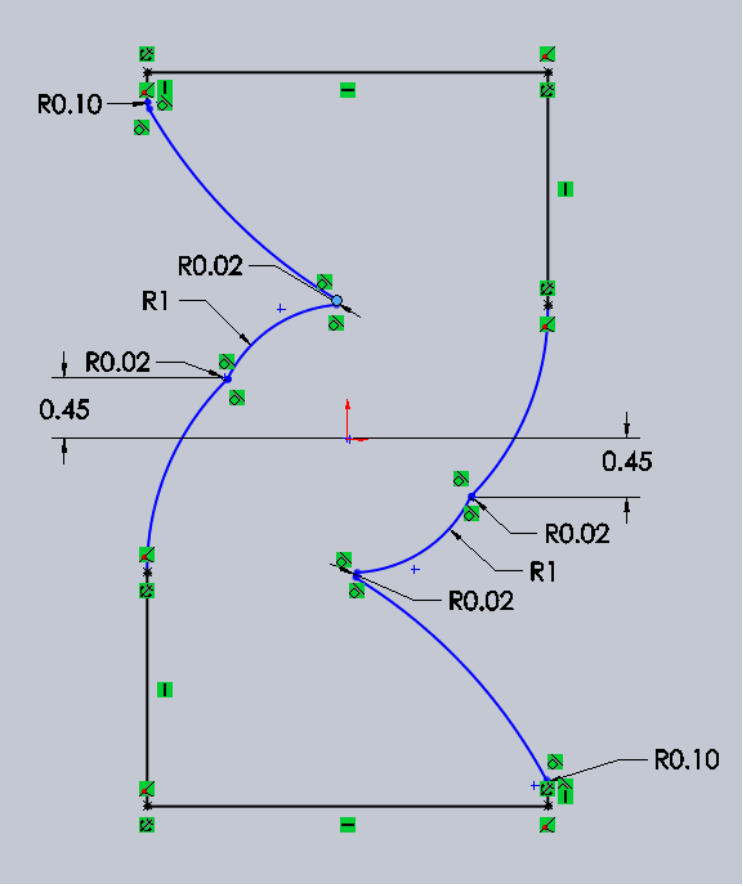


Figure 27 Using smart dimension to fix arc radii

Complete the sketch by clicking **Accept Sketch.**

C. Extrude the sketch into 3D.

1. In the Explorer Bar click the **Features** tab > **Extruded Boss/Base** (make sure that Sketch 1 is selected before you click on the **Extruded Boss/Base** button).
2. For the thickness enter 0.1 meters. Click the green check mark to accept.

D. Design the center of the envelope for the rotor.

1. In the **Design Tree**, click **Front Plane**. In the Explorer Bar, click the **Sketch** tab > **Sketch.**
2. A new item should appear in the **Design Tree** called **sketch2**.
3. Click the **Circle** feature from the explorer bar and create a circle about the origin with radius equal to 0.99 meters. Click the green check to accept.
4. Click **Accept** in the top right corner of the layout.

E. Make a cut out of the Envelope with **sketch2.**

1. With **sketch2** selected click on the **Features** tab in the Explorer Bar and then **Extruded Cut**.
2. Change the distance measure to 0.1 meters. A yellow circle should appear in the middle of the envelope where **sketch2** exists. If this is not the case change the direction of the cut so that the yellow circle appears. Click the green check mark.

F. Save the file as **Envelope.sldprt**. Then select **Save As** and save it a second time as a Parasolid file named **Envelope.x_t**.

THIS PAGE INTENTIONALLY LEFT BLANK

# APPENDIX F. ROTOR GEOMETRY GENERATION

A. Launch **SolidWorks 2010**.

1. In the **SolidWorks** Banner, Select **File > New Project** from the Main Menu and click on **Part – a 3D representation of a single design component > OK.**
2. In the **SolidWorks** Banner, Select **Tools > Options > Document Properties – Units.** Ensure that **MKS (meter, kilogram, second)** is selected.

B. Draw 2D Rotor.

1. Disc Creation
    a. Click on the blue **Z-Plane** arrow in the bottom left of the window.
    b. Right click on the **Front Plane** in the design tree on the left side of the window and choose the **Sketch** feature.
    c. Click on the **Draw a Circle** feature. Make the circle have a radius of 1m. Click the green check mark and click **Exit Sketch**.

C. Extrude the sketch into 3D.

1. In the Explorer Bar click the **Features** tab > **Extruded Boss/Base** (make sure that Sketch 1 is selected before you click on the **Extruded Boss/Base** button).
2. For the thickness enter 0.1 meters. Click the green check mark to accept.

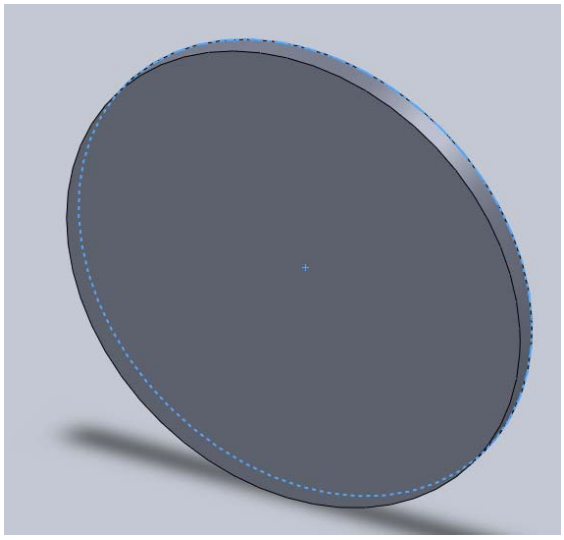

Figure 28 Rotor disc

D. Blade Creation.

1. Click on the blue **Z-Plane** arrow in the bottom left of the window.
2. Right click on the **Front Plane** in the design tree on the left side of the window and choose the **Sketch** feature.
3. Click on the **Point** feature to sketch a point. Both points are to be fixed. This is done by clicking the **Fix** icon while inputting the points.

| Point | X Parameter (m) | Y Parameter (m) |
|---|---|---|
| **1** | **0** | **0.7** |
| **2** | **0** | **0.95** |

Table 5. Blade point parameters

a. Draw 3-point arcs connecting the two points.

b. Connect the two points together with the 3-point arc. Set the radius to 0.2m

c. Connect the two points together again with the 3-point arc. Set the radius to 0.3m

| 3-Point Arc | Radius (m) |
|---|---|
| 1 | 0.2 |
| 2 | 0.3 |

Table 6. Rotor design arc parameters

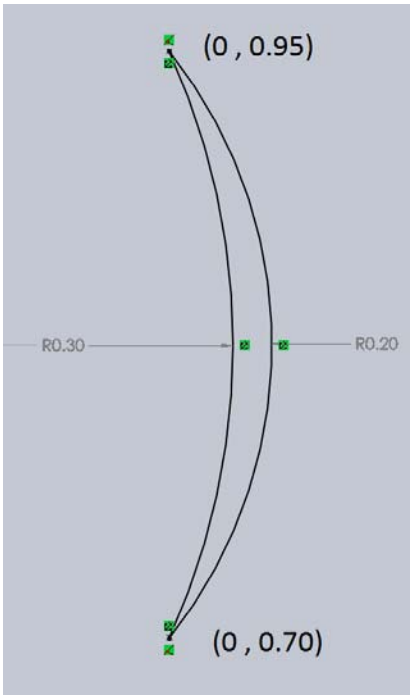


Figure 29 Rotor blade shape

4. Soften the edges of the curves by adding a **Fillet** at the important junctures.
   a. Click the **Fillet** feature. While holding down the **CTRL** key, select both lines on either side of the connections enumerated above. Once selected, enter the **Fillet Parameters** as listed in the table.

| Fillet | Fillet Parameter (m) |
|---|---|
| 1 | 0.0005 |
| 2 | 0.0005 |

Table 7. Rotor fillet parameters

5. Create a Circular Sketch Pattern
    a. Left click the mouse button and drag over the entire sketch before releasing the left button. The sketch should be highlighted in blue.
    b. On the tool bar above the sketch click the pull down tab next to **Linear Sketch Pattern.** Select **Circular Sketch Pattern**.
    c. For number of occurrences enter 25 and click the green checkmark. Exit the sketch.

E. Make a cut out of the Envelope with **sketch2.**

3. With **sketch2** selected click on the **Features** tab in the Explorer Bar and then **Extruded Cut**.
4. Change the distance measure to 0.1 meters. Blades should appear cut through the disc where **sketch2** exists. If this is not the case change the direction of the cut so that the yellow blades appear. Click the green check mark.

F. Save the file as **Rotor.sldprt**. Then select **Save As** and save it a second time as a Parasolid file named **Rotor.x_t**.

# LIST OF REFERENCES


[1] J. McDonaugh, 2011, "Facts About Water Mills," from http://www.ehow.com/info_8498789_water-mills.html

[2] H. Olgun, 1998, "Investigation of the performance of a cross-flow turbine," *International Journal of Energy Research*, vol. 22, 953–964.

[3] N. M. Aziz and V. R. Desai, "An experimental study of the effect of some design parameters on crossflow turbine efficiency," Internal Report for Department of Energy, Bonneville Power Administration, Portland, Oregon, from http://www.frenchriverland.com/a_laboratory_study_to_improve_the_efficiency_of_cross-flow_turbines-_nadim_aziz_&_venkappayya.htm

[4] Nova Scotia Power, from http://www.nspower.ca/en/home/environment/renewableenergy/tidal/annapolis.aspx

[5] J. Thomas, 2007, "1.2 Megawatts: World's Largest Tidal Turbine to be Installed." From http://www.treehugger.com/renewable-energy/12-megawatts-worlds-largest-tidal-turbine-to-be-installed.html

[6] R. Black, 2011, "India plans Asian tidal power first." from http://www.bbc.co.uk/news/science-environment-12215065

[7] Lunar Energy, from http://www.lunarenergy.co.uk/index.htm

[8] Tidal Energy Pty Ltd, from http://tidalenergy.net.au/

[9] A. N. Gorban, A. M. Gorlov, and V. M. Silantyev, "Limits of the Turbine Efficiency for Free Fluid Flow." from http://www.math.le.ac.uk/people/ag153/homepage/Gorlov2001.pdf

THIS PAGE INTENTIONALLY LEFT BLANK

# BIBLIOGRAPHY


BBC News, 2008, “Tidal Energy System on Full Power.” from http://news.bbc.co.uk/2/hi/uk_news/northern_ireland/7790494.stm

Sustainable Bristol, 2011, “Bristol’s Tidal Energy Growth Continues.” from http://www.sustainablebristol.com/2011/12/bristol%E2%80%99s-tidal-energy-growth-continues/

Chang J., 2008, “Hydrodynamic Modeling and Feasibility Study of Harnessing Tidal Power at the Bay of Fundy.” from http://digitallibrary.usc.edu/assetserver/controller/item/etd-Chang-20080312.pdf

Kirke B., 2005, “Developments in Ducted Water Current Turbines.” from http://www.cyberiad.net/library/pdf/bk_tidal_paper25apr06.pdf

Rudolf J. C., 2010, “Prince of Tides: A Mammoth Turbine.” from http://green.blogs.nytimes.com/2010/08/13/the-prince-of-tides-a-mammoth-turbine/

Clean Current, “The Race Rocks Tidal Energy Project.” from http://www.cleancurrent.com/technology/rrproject.htm

Severn Estuary Partnership, “The Estuary.” from http://www.severnestuary.net/sep/resource.html

Fairley P., 2007, “Tidal Turbines Help Light Up Manhattan.” from http://www.technologyreview.com/Energy/18567/

Carrell S., 2011, “Wave and Tidal Power Almost Ready for Mass Consumption, says Alex Salmond.” from http://www.guardian.co.uk/environment/2011/sep/27/wave-and-tidal-power-alex-salmond

World Energy Council, 2007, “Survey of Energy Resources 2007.” from http://www.worldenergy.org/publications/survey_of_energy_resources_2007/tidal_energy/754.asp

Shiono M., Suzuki K., and Kiho S., 2002, “Output Characteristics of Darriens Water Turbine with Helical Blades for Tidal Current Generations,” The Twelfth International Society of Offshore and Polar Engineering Conference, 2002, pp. 859–864.

THIS PAGE INTENTIONALLY LEFT BLANK

# INITIAL DISTRIBUTION LIST

1. Defense Technical Information Center
   Ft. Belvoir, Virginia

2. Dudley Knox Library
   Naval Postgraduate School
   Monterey, California

3. Prof. Garth V. Hobson
   Department of Mechanical and Aeronautical Engineering
   Naval Postgraduate School
   Monterey, California

4. Prof. Anthony J. Gannon
   Department of Mechanical and Aeronautical Engineering
   Naval Postgraduate School
   Monterey, California

5. Karen A. Flack
   Department of Mechanical Engineering
   United States Naval Academy
   Annapolis, Maryland